

Promiscuous Methionyl-tRNA Synthetase Mediates Adaptive Mistranslation against Oxidative Stresses

Jin Young Lee¹, Dae Gyu Kim¹, Byung-Gyu Kim¹, Won Suk Yang¹, Jeena Hong¹, Taehee Kang¹, Young Sun Oh¹, Kyung Rok Kim², Byung Woo Han², ByungJoon Hwang³, BeomSik Kang⁴, Mi-Sun Kang⁵, Myung-Hee Kim⁵, Nam Hoon Kwon^{1*} and Sunghoon Kim^{1,6*}

¹Medicinal Bioconvergence Research Center, College of Pharmacy, Seoul National University, Seoul 151-742, Korea. ²Research Institute of Pharmaceutical Sciences, Department of Pharmacy, College of Pharmacy, Seoul National University, Seoul 151-742, Korea. ³Department of Molecular Bioscience, Kang Won National University, Chuncheon-si, Gangwon-do, 200-701, Korea. ⁴School of Life Science and Biotechnology, Kyungpook National University, Daegu, 702-701, Korea. ⁵Department of Computer Science and Engineering Center for Computer Graphics and Virtual Reality, Ewha Womans University, Seoul 120-750, Korea. ⁶WCU Department of Molecular Medicine and Biopharmaceutical Sciences, Graduate School of Convergence Science and Technology, Seoul National University, Suwon 443-270, Korea.

*Authors for correspondence (nanarom1@snu.ac.kr; sungkim@snu.ac.kr)

1 **ABSTRACT**

2 Aminoacyl-tRNA Synthetases (ARSs) acylate tRNAs with amino acids. Charging
3 tRNAs with the right amino acids is the first step in translation; therefore, the accurate
4 and error-free functioning of ARSs is an essential prerequisite for translational fidelity.
5 A recent study found that methionine (Met) can be incorporated into non-Met residues
6 of proteins through methionylation to non-cognate tRNAs under oxidative stress.
7 However, it was not understood how this mis-methionylation is achieved. Here, we
8 report that methionyl-tRNA synthetase (MRS) is phosphorylated at Ser209 and Ser825
9 by extracellular signal-related kinase (ERK) upon reactive oxygen species (ROS) stress,
10 and that this phosphorylated MRS showed increased affinity to non-cognate tRNAs
11 with lower affinity to tRNA^{Met}, leading to an increase in Met residues in cellular
12 proteins. The expression of a mutant MRS containing the substitutions S209D and
13 S825D, mimicking dual phosphorylation, reduced ROS levels and cell death. This
14 controlled inaccuracy of MRS seems to serve as a defense mechanism against ROS-
15 mediated damage at the cost of translational fidelity.

16
17
18
19
20
21
22
23
24
25
26
27
28
29
30
31
32

33 **INTRODUCTION**

34 Reactive oxygen species (ROS), which are generally unstable and highly reactive, are
35 continuously produced because of normal physiological events such as aerobic
36 metabolism as well as extracellular stress including radiation or chemicals. Low levels
37 of ROS promote cellular proliferation and differentiation, but long-term or high-level
38 exposure to ROS induces oxidative damage, causing cell death. Maintaining redox
39 homeostasis is therefore essential for normal cell growth and survival (Trachootham et
40 al., 2009). Conversely, an ROS imbalance is related to several pathophysiological
41 conditions, including cancer, diabetes, chronic inflammation, atherosclerosis, ischemia-
42 reperfusion injury, and neurodegenerative disorders (Jones et al., 2012; Waris and Ahsan,
43 2006).

44 To protect against oxidative damage, cells have recruited various endogenous
45 enzymatic and non-enzymatic antioxidants, including peroxidase, superoxide dismutase,
46 glutathione, NADPH, ubiquinone, vitamin, and carotenoids (Birben et al., 2012). Apart
47 from these antioxidant molecules, a distinct antioxidant mechanism uses methionine
48 (Met) as a ROS scavenger to protect proteins (Luo and Levine, 2009). Met residues on
49 the surface of proteins intercept ROS such as hydrogen peroxides and they are
50 converted to methionine sulfoxides. The oxidized Met is then reduced to Met by
51 methionine sulfoxide reductases (Levine et al., 1996; Levine et al., 2000; Luo and
52 Levine, 2009; Stadtman et al., 2002; Stadtman et al., 2003).

53 It was recently shown that methionylation to non-cognate tRNAs, termed ‘Met-
54 misacylation’, increased up to 10% in mammalian cells under oxidative stress (Netzer et
55 al., 2009; Wiltrout et al., 2012). This Met-misacylation predominantly occurs in tRNA
56 families that originally carry charged or polar amino acids (Netzer et al., 2009),
57 implying that methionyl-tRNA synthetase (MRS) might be involved in Met-
58 misacylation to non-cognate tRNAs such as tRNA^{Lys}, tRNA^{Gly} and tRNA^{Leu} (Netzer et
59 al., 2009). However, the molecular mechanism responsible for Met-misacylation under
60 oxidative stress remains unidentified.

61 MRS is an enzyme responsible for the ligation of Met to the cognate initiator or
62 elongator tRNA^{Met}. In the mammalian system, MRS is normally bound to the multi-
63 tRNA synthetase complex (MSC), making specific interaction with aminoacyl-tRNA
64 synthetase (ARS)-interacting multifunctional protein 3 (AIMP3/p18) (Park et al., 2005).

65 Our recent study suggests that affinity to the cognate tRNA is reduced by MRS
66 phosphorylation, resulting in suppression of global translation (Kwon et al., 2011). This
67 study suggested that the tRNA binding affinity of MRS can be modulated by post-
68 translational modification. Further expanding this discovery, we hypothesized that
69 certain modifications of MRS could alter its tRNA specificity and induce Met-
70 misacylation to non-cognate tRNAs, which would serve as a protective mechanism
71 against oxidative stress. In this study, we investigated the functional significance of
72 MRS in protection against ROS damage and in the molecular mechanism that controls
73 the specificity of tRNA recognition.

74

75 **RESULTS**

76 **MRS is phosphorylated by extracellular signal-related kinase (ERK) under** 77 **oxidative stress**

78 Based on previous studies showing the possibility of MRS-mediated Met-misacylation
79 (Jones et al., 2011; Netzer et al., 2009; Wiltrout et al., 2012) and modulation of MRS
80 catalytic activity by phosphorylation (Kwon et al., 2011; Pendergast and Traugh, 1985),
81 we first examined MRS modification under ROS stress. Protein extracts from HeLa
82 cells treated with arsenite, a ROS-inducing agent, were separated by 2 dimensional-
83 polyacrylamide gel electrophoresis (2D-PAGE) and then immunoblotted using the anti-
84 MRS antibody. Additional spots of MRS were generated on the acidic side by treatment
85 with arsenite; these spots disappeared after alkaline phosphatase treatment, indicating
86 that MRS was phosphorylated under ROS stress (Fig. 1A). To identify which amino
87 acid residues were involved in ROS-mediated phosphorylation, proteins from control
88 and ROS-induced HeLa cells were immunoprecipitated with anti-MRS antibody and
89 immunoblotted with phospho-specific antibodies. Phosphorylation of MRS at serine
90 residues was observed in MRS extracted from arsenite-treated cells (Fig. 1B), whereas
91 phosphorylation at threonine or tyrosine residues was not detected. Serine-specific
92 phosphorylation was also confirmed in H₂O₂-treated HeLa cells (Fig. S1A). Removal of
93 ROS by treatment with diphenyleneiodonium (DPI), a broad inhibitor of oxidases,
94 apparently reduced the arsenite-dependent phosphorylation of MRS (Fig. 1C),
95 indicating that kinases activated under ROS signaling would be involved in MRS
96 phosphorylation. Since mitogen-activated protein kinases (MAPKs) are well known for

97 their various functions upon stimulation by ROS (Lau et al., 2004; Pan et al., 2009; Son
98 et al., 2011), we treated HeLa cells with MAPK-specific inhibitors and monitored MRS
99 phosphorylation. Serine-specific phosphorylation of MRS induced by arsenite was
100 dramatically suppressed in cells treated with the ERK inhibitor PD98059, whereas p38
101 MAPK or c-Jun N-terminal kinase (JNK) inhibitors did not influence MRS
102 phosphorylation (Fig. 1D). Next, we performed an *in vitro* kinase assay by incubating
103 glutathione sulfotransferase (GST) or GST-MRS with purified active ERK and [γ -
104 32 P]ATP to confirm whether MRS is a real substrate for ERK. GST-MRS, but not GST,
105 showed obvious phosphorylation signal by ERK (Fig. 1E); therefore, we concluded that
106 MRS was phosphorylated at serine residues by ERK under ROS stress.

107

108 **Determination of ERK-induced phosphorylation sites in MRS**

109 Human MRS consists of three functional domains, the GST-like (MD1, residues 1–266),
110 catalytic (MD2, residues 267–597), and tRNA-binding (MD3, residues 598–900)
111 domains (Fig. 1F). Using these domain fragments, we conducted an *in vitro* kinase
112 assay to narrow down the ERK-mediated phosphorylation domain of MRS. Since a
113 strong phosphorylation signal was observed in MD1 and MD3, but not in MD2 (Fig.
114 1G), we analyzed phosphorylation sites in MD1 and MD3 after the *in vitro* kinase assay
115 by mass spectrometry to determine the ERK-dependent phosphorylation site in MRS.
116 Among the phosphorylation sites of MRS detected (Fig. S2A), we selected the serine
117 residues Ser209 and Ser825, because ROS-induced MRS phosphorylation is serine-
118 specific (Fig. 1B). We synthesized biotinylated MRS peptides containing Ser209 and
119 Ser825, respectively, as well as the same peptides with serine to alanine substitution.
120 The peptide kinase assay revealed the apparent phosphorylation of both Ser209- and
121 Ser825-containing peptides by ERK, whereas little signal was observed in alanine-
122 substituted mutant peptides (Fig. 1H, left) or ERK inhibitor-treated conditions (Fig. 1H,
123 right). The same results were obtained when the *in vitro* kinase assay was performed
124 with wild-type (WT) and mutant GST-MRS proteins. The GST-MRS S209A/S825A
125 (SA) mutant, in which both serine residues were substituted with alanines, showed
126 minimal phosphorylation upon incubation with ERK, compared with WT MRS (Fig. 1I).
127 We also transfected HEK293T cells with WT Myc-MRS or the Myc-MRS SA mutant
128 and analyzed serine-specific phosphorylation by immunoblotting. The phosphorylation

129 signal was increasingly detected in WT MRS by arsenite treatment, but was not detected
130 in the dual alanine-substituted SA mutant (Fig. 1J). Moreover, H₂O₂ treatment did not
131 induce phosphorylation in the MRS SA mutant (Fig. S1A). We also checked the
132 phosphorylation state in single alanine-substituted mutants. Although the serine-specific
133 phosphorylation signal was slightly lower in the S209A and S825A single mutants
134 compared to WT MRS, these single alanine-substituted mutants did not show a dramatic
135 decrease as seen with the MRS SA mutant, suggesting that the Ser209 and Ser825
136 residues are dually phosphorylated by ERK under ROS stress (Fig. S2B).

137 ERK is activated upon various stimuli including UV, therefore we wondered
138 whether Ser209 and Ser825 phosphorylation is specific to ROS. We transfected Myc-
139 MRS S662A into HEK293T cells along with Myc-MRS WT and investigated MRS
140 phosphorylation. Ser662 residue of MRS is known to be phosphorylated by general
141 control nonderepressible 2 (GCN2) upon UV irradiation (Kwon et al., 2011). If Ser209
142 or Ser825 can be phosphorylated by UV-activated ERK, phosphorylation signal will be
143 detected in MRS S662A by UV. Phosphorylation of MRS S662A, however, was only
144 detected under ROS stress but not by UV suggesting that Ser209 and Ser825
145 phosphorylation is specific to ROS stress (Fig. S2C).

146

147 **Phosphorylation of MRS at Ser209 and Ser825 induces Met-misacylation under** 148 **ROS stress**

149 Because MRS was modified by phosphorylation under ROS stress, we investigated the
150 correlation between Met-misacylation and the dual phosphorylation of MRS under ROS
151 stress conditions. We first analyzed circular dichroism (CD) spectra of WT MRS, the
152 MRS SA mutant and the S209D/S825D (SD) mutant and observed a temperature-
153 dependent structural change of MRS SD mutant in the far-UV spectra (Fig. 2A). To
154 evaluate the Met-misacylation ability of the MRS SD mutant, we performed *in vitro*
155 tRNA binding and aminoacylation activity assays. Based on a previous report
156 suggesting that ROS-dependent Met-misacylation predominantly occurs in
157 tRNA^{Lys}(CUU) (Netzer et al., 2009), we tested tRNA^{Lys}(CUU) first. We examined the
158 interaction between the MRS SD mutant and tRNA^{Lys}(CUU) via electrophoretic
159 mobility shift assay (EMSA). The MRS SD mutant showed clearly increased
160 association with radioactively labeled tRNA^{Lys}(CUU) in a dose-dependent manner,

161 whereas WT MRS did not (Fig. 2B, top). Both WT MRS and the SD mutant interacted
162 with elongator tRNA^{Met} (tRNA^{eMet})(CAU) to a similar extent (Fig. 2B, bottom).

163 In the aminoacylation activity assay, the K_M value of the MRS SD mutant for
164 tRNA^{Lys}(CUU) was about six-fold higher than that of WT MRS for tRNA^{eMet}(CAU)
165 (Table 1). It is notable that the MRS SD mutant showed relatively higher affinity to
166 tRNA^{Lys}(CUU) rather than to tRNA^{eMet}(CAU), whereas the K_M of WT MRS for
167 tRNA^{Lys}(CUU) was not measurable. Although MRS SA mutant showed significant
168 decrease in its catalytic activity to tRNA^{Met}, it retained its specificity to the cognate
169 tRNA. We further confirmed the Met-misacylation ability of the MRS SD mutant to
170 other types of tRNA such as tRNA^{Ala}(AGC), tRNA^{Gly}(GCC), tRNA^{His}(GUG), and
171 tRNA^{Leu}(CAG). The MRS SD mutant generally showed considerable binding affinities
172 to these non-cognate tRNAs compared with WT MRS (Fig. S3A). Consistently, the
173 MRS SD mutant charged non-cognate tRNAs with Met at levels similar to those seen
174 with tRNA^{eMet}(CAU), with the highest activity for tRNA^{Lys}(CUU) among the tRNAs
175 (Fig. S3B). These results suggested that dual phosphorylation of MRS at residues
176 Ser209 and Ser825 can endow MRS with the ability to recognize non-cognate tRNAs
177 and misacylate them with Met.

178 Next, we investigated whether Met-misacylated tRNA families can be used for
179 translation. Since MRS incorporation into the MSC may affect translational efficiency,
180 we firstly performed immunoprecipitation assay using anti-EPRS (glutamyl-prolyl
181 tRNA synthetase) and anti-Myc antibodies to see the existence of the Myc-MRS SD
182 mutant in the MSC. EPRS, the representative subunit of the MSC, and the Myc-MRS
183 SD mutant were co-immunoprecipitated together, therefore we concluded that
184 exogenous MRS SD mutant can be localized in the MSC like endogenous MRS (data
185 not shown). We set up a fluorescence system using TagRFP to monitor Met-
186 misacylation. TagRFP is a red fluorescent protein whose Met67 residue is critical for its
187 fluorescence. We mutated the ATG codon for Met67 to AAG for Lys to turn off the
188 fluorescence and observed that the red fluorescence signal from the TagRFP M67K
189 mutant was undetectable (Fig. 3A). If MRS mismethionylated tRNA^{Lys}(CUU), then
190 Met-tRNA^{Lys}(CUU) could be incorporated into the mutated codon of TagRFP M67K to
191 restore the Lys residue to original Met, thereby restoring red fluorescence. We
192 transfected the TagRFP M67K mutant together with empty vector (EV), WT Myc-MRS,

193 the Myc-MRS SA mutant, or the Myc-MRS SD mutant into HEK293T cells. EV-, WT
194 MRS-, and MRS SA-expressing cells exhibited increased red fluorescence signal upon
195 arsenite treatment, with the most enhanced fluorescence in WT MRS-expressing cells
196 (Fig. 3B). The MRS SD mutant showed increased fluorescence signal regardless of
197 arsenite treatment (Fig. 3B). Based on the results of immunoblotting, this difference in
198 fluorescence among the MRS proteins was not due to the expression level of TagRFP
199 (Fig. 3C). We analyzed the images based on the fluorescence-positive cell number (Fig.
200 3D) as well as fluorescence intensity (Fig. 3E). Both of these results suggested three
201 notable points: 1) ROS-responsive Met-misincorporation by endogenous and exogenous
202 WT MRS; 2) similar increase in Met-misincorporation under ROS condition in the cells
203 expressing EV or the MRS SA mutant; and 3) basally enhanced Met-misincorporation
204 by the MRS SD mutant. Similar patterns were also observed with the TagRFP M67H
205 and M67G mutants, proving the MRS-mediated production of Met-tRNA^{His}(GUG) and
206 Met-tRNA^{Gly}(UCC) and their incorporation into the TagRFP mutant protein,
207 respectively (Fig. S3C).

208 To further investigate the possible residue positions of a protein at which Met
209 can be misincorporated, we first transfected HEK293T cells with the pBiFC-VN173-
210 AIMP3 vector (Kwon et al., 2011) to use the Flag-VN (N-terminal fragment of Venus)-
211 AIMP3 protein as a reporter for monitoring Met-misincorporation. We chose Flag-VN-
212 AIMP3 because this protein is small (347 net amino acids without linker) and contains a
213 relatively small number of Met residues (4 amino acids). Flag-VN-AIMP3 was
214 immunoprecipitated after the addition of [³⁵S]Met to the cells, and the autoradioactivity
215 emanating from the Flag-VN-AIMP3 was detected (Fig. 3F,G). The radioactive signal
216 from Flag-VN-AIMP3 was increased upon arsenite treatment, whereas the enhanced
217 signal disappeared upon treatment with ERK inhibitor (Fig. 3F). This signal was not
218 observed by serum stimulation either, which is another activation signal for ERK,
219 suggesting that Met-misincorporation is a phenomenon specifically occurs upon ROS
220 stress (data not shown). We also confirmed MRS-dependent [³⁵S]Met incorporation into
221 Flag-VN-AIMP3 in HEK293T cells expressing EV, WT MRS, the SA or SD mutant.
222 Autoradioactivity was detected in the protein isolated from arsenite-treated HEK293T
223 cells with different signal intensity according to the expressional and mutational status
224 of MRS. MRS WT-transfected cells showed the topmost signal intensity of ROS-

225 dependent Met-misincorporation among the EV, WT, and the SA mutant expressing
226 cells (Fig. 3G). The MRS SD mutant induced the production of radioactive Flag-VN-
227 AIMP3 regardless of arsenite or ERK inhibitor treatment (Fig. 3G). This Met-
228 misincorporation under ROS stress was MRS specific because leucine-misincorporation
229 into Flag-VN-AIMP3 was not observed by overexpression of leucyl-tRNA synthetase
230 (LRS) (Fig. S3D). To further validate the MRS-mediated Met-misincorporation, we
231 immunoprecipitated Flag-VN-AIMP3 from HEK293T cell lysates and analyzed the
232 Met-misincorporated residues using mass spectrometry. We identified several peptides
233 containing Met at non-Met residue positions in the MRS SD-expressing cells, although
234 there was basal Met-misacylation in WT HEK293T cells (Table 2; Fig. 4; Fig. S4).
235 Interestingly, residues swapped with Met were detected on the surface of AIMP3 as
236 well as Venus (Fig. 4A,B). In addition, the swapped residues of AIMP3 do not
237 participate in the MRS interaction, and they are expected to be exposed outside of the
238 MSC (Fig. 4A, bottom). This supports the idea that Met-misincorporation is not an
239 accidental event, but it results in relocating Met on the surface of proteins as a ROS
240 scavenger.

241

242 **MRS-mediated Met-misacylation reduces intracellular ROS levels and protects** 243 **cells from oxidative damage**

244 Since residue switching with Met was detected on the protein surface where ROS
245 attacks vulnerable amino acids, we examined whether MRS-mediated Met-misacylation
246 can actually reduce intracellular ROS levels by using the dichloro-dihydro-fluorescein
247 diacetate (DCFH-DA) assay. Whereas EV-expressing control cells or MRS SA mutant-
248 expressing cells showed a little bit increased ROS levels upon arsenite treatment, WT
249 MRS- and SD mutant-expressing cells did not (Fig. 5A). It is known that ROS increases
250 pro-apoptotic Bax while reducing the expression level of Bcl-2, the Bax inhibitor (Chen
251 et al., 1998; Fleury et al., 2002; Hossain et al., 2000). Thus, we checked the expression
252 levels of these markers and found that cells expressing WT MRS and the SD mutant
253 were more resistant to apoptotic cell death upon arsenite-induced ROS generation than
254 EV- or MRS SA mutant-expressing cells (Fig. 5B). Together, these results suggest that
255 MRS phosphorylation at Ser209 and Ser825 can reduce intracellular ROS level
256 resulting in cell protection from ROS-mediated apoptosis.

257 To investigate the effect of MRS-mediated Met-misacylation on cell survival,
258 we performed the 3-(4,5-dimethylthiazol-2-yl)-2,5-diphenyltetrazolium bromide (MTT)
259 assay. First, we reduced the expression level of MRS using siRNA treatment. MRS
260 knockdown significantly reduced the cell viability under ROS stress suggesting the
261 critical role of MRS in cell protection against ROS stress (Fig. 5C). Overexpression of
262 WT MRS or the MRS SD mutant under ROS stress, whether transient (Fig. 5D) or
263 stable (Fig. 5E), maintained cell survival at levels similar to that of normal growth in the
264 MTT assay. In contrast, the MRS SA mutant could not protect cells from oxidative
265 damage as much as MRS WT or the SD mutant did, resulting in significant reduction in
266 cell viability as shown in ROS-treated control cells. Growth curve analysis also showed
267 the same results as in the MTT assay. ROS retarded the growth of stable HeLa cells
268 expressing EV and the MRS SA mutant by up to 23.14% and 23.62%, respectively, but
269 it did not cause any significant effects on the growth of stable HeLa WT and SD mutant
270 cells (Fig. 5F). A similar pattern of cell viability under ROS stress was also observed
271 with H₂O₂ treatment (Fig. S1B). Moreover, the terminal deoxynucleotidyl transferase
272 dUTP nick end labeling (TUNEL) assay indicated that cells expressing MRS WT or SD
273 mutant were more resistant to apoptosis upon ROS stimuli than EV or MRS SA-
274 expressing cells (Fig. 5G). The cell protective effect of MRS WT under ROS stress was
275 significantly reduced by U0126 suggesting that ERK activation is required for the cell
276 protective function of MRS (Fig. 5H; Fig. S3E). In addition, unlike MRS, LRS
277 overexpression did not compensate for the reduced cell viability caused by ROS (Fig.
278 S3F). These results indicate that dual phosphorylation of MRS is critical for cell
279 protection against oxidative damage.

280 In summary, under oxidative stress conditions, MRS is phosphorylated at
281 Ser209 and Ser825 by activated ERK. Dually phosphorylated MRS induces Met-
282 misacylation of noncognate tRNAs. Increased numbers of Met residues via
283 misincorporation during translation can serve as ROS scavengers and protect cells from
284 ROS-induced damage and apoptosis (Fig. 6).

285

286 **DISCUSSION**

287 Previous studies reported the importance of the Met residue as an antioxidant agent
288 (Levine et al., 1996; Luo and Levine, 2009; Stadtman et al., 2002; Stadtman et al.,

289 2003) and an increase in Met-misacylation and Met-misincorporation under ROS stress
290 (Netzer et al., 2009). Although MRS mutation- or MRS condition-dependent Met-
291 misacylation was identified in *Escherichia coli* and *Saccharomyces cerevisiae* (Jones et
292 al., 2011; Wiltrout et al., 2012), the exact mechanism and meaning of this phenomenon
293 in human cells is not yet understood. In this study, we identified human MRS as a new
294 substrate for ERK under ROS stress and demonstrated a novel function of
295 phosphorylated MRS, changing tRNA specificity to increase the rate of codon-
296 independent Met-mistranslation during oxidative damage.

297 Accurate translation is an important issue for cells to maintain their normal
298 cellular integrity (Yadavalli and Ibba, 2012). To maintain translational fidelity, ARSs
299 possess an editing function: they remove misactivated aminoacyl-adenylate or
300 mischarged tRNAs via several mechanisms. While other class Ia ARSs have at least one
301 connecting peptide 1 (CP1) with an editing site, and perform pre-transfer and post-
302 transfer editing, MRS has a truncated CP1 domain and performs pre-transfer editing in a
303 catalytic site-dependent manner (Englisch et al., 1986; Fersht and Dingwall, 1979;
304 Jakubowski, 1991; Yadavalli and Ibba, 2012). Although the manner in which human
305 MRS carries out its editing function and recognizes its cognate tRNA is structurally
306 unclear, it is known that bacterial MRS recognizes the anticodon region and acceptor
307 A73 in tRNA^{Met} (Senger et al., 1992). In eukaryotes, MRS is expected to have a certain
308 additional mode for the recognition and aminoacylation of tRNA. First, the C-terminal
309 WHEP (824–900 amino acids) domain strengthens the association of tRNA^{Met} to MRS
310 under suboptimal tRNA concentrations (Kaminska et al., 2001). Second, the N-terminal
311 215–267 amino acids on the GST-like domain are critical for MRS catalytic activity (He
312 et al., 2009). Our results are in line with these studies in that phosphorylation in these
313 appended domains, but not in the core domain, can modulate MRS enzymatic activity.
314 The structural change in the MRS SD mutant also supports the possibility of functional
315 modulation by MRS modification (Fig. 2A). Although further investigation is required
316 to understand the interaction of phosphorylated MRS with a non-cognate tRNA, it does
317 not seem to recognize either the anticodon region or the discriminator base in the non-
318 cognate tRNAs. The common bases between Met-misacylated tRNAs and tRNA^{Met} are
319 mainly located in the D and T ψ C arms, implying that phosphorylated MRS may
320 recognize tRNAs in a different way.

321 WT MRS and the SD mutant showed similar levels of tRNAe^{Met} binding in
322 EMSA, whereas their kinetic analyses suggested that MRS SD mutant charges
323 tRNAe^{Met} less efficiently than WT MRS does (Table 1; Fig. 2B). The MRS SD mutant,
324 on the other hand, showed more effective aminoacylation activity to tRNA^{Lys}.
325 Considering only the Met-charging efficacy, the reduced susceptibility of
326 phosphorylated MRS to tRNAe^{Met} is unnecessary. The reduced affinity to the cognate
327 tRNAe^{Met} may be an inadvertent result of the increased selectivity to other tRNAs. The
328 activity of MRS SD mutant to the tRNAi^{Met}, however, was similar to that of MRS WT
329 indicating that MRS phosphorylation under ROS stress may not cause adverse effect on
330 translation initiation. Indeed, there was little difference between the overexpression of
331 MRS WT and the SD mutant in their effect on global translation (data not shown).

332 Although MRS SD mutant revealed evident charging activity to tRNA^{Lys}, MRS
333 may have to compete with lysyl-tRNA synthetase (KRS) for capturing tRNA^{Lys} under
334 ROS stress unless there is spare tRNA^{Lys}. We analyzed free tRNA^{Lys} as well as charged
335 tRNA^{Lys} using acidic urea PAGE gel and observed that some portion of free tRNA^{Lys}
336 seems available even when KRS is fully active (data not shown). It also implies the
337 availability of other spare non-cognate tRNAs for misacylation. Met-misincorporation
338 does not require high amounts of other tRNAs. It is known that total increase of Met-
339 misincorporation is about 10% under ROS stress (Netzer et al., 2009). Also other
340 possibilities to increase the tRNAs availability under oxidative stress, such as the
341 accessibility changes of the tRNAs to their cognate ARSs, cannot be excluded.

342 Considering that a series of tRNAs that mainly carry charged or polar amino
343 acids are mismethionylated under ROS stress (Netzer et al., 2009), the shift in substrate
344 preference can confer apparent merits to cells, such as relocation of Met residues on the
345 surface and an increased number of Met residues. According to Levine *et al.*, all the Met
346 residues in the original positions are not used as ROS scavenger (Levine et al., 1996).
347 About 50% of the original Met residues in glutamine synthetase were oxidized by ROS,
348 with the intact Met residues being buried within the core of protein. When repositioned
349 in exposed spots with increased occupancy by misacylation, Met has a greater chance of
350 reacting with ROS. In fact, the Met-misincorporated residues in Flag-VN-AIMP3 were
351 all detected on the surface of protein, supporting this point of view (Fig. 4). Met-
352 misincorporation increased the number of Met residues from the original 3 to 11 in VN

353 (173 amino acids) and from 1 to 8 in AIMP3 (174 amino acids) (Table 2; Fig. 4).

354 Cells under normal conditions also had a basal level of Met-misincorporation
355 on the protein surface (Fig. 3B; Fig. 4). This is probably due to endogenous ROS levels.
356 Interestingly, the residues basally exchanged with Met were not perfectly matched up to
357 those detected under MRS SD expression. This suggests that Met-misacylation by MRS
358 can be arbitrary in some respects but can provide equal results under independent
359 circumstances. This is probable due to the characteristics of non-cognate tRNAs, which
360 can be used as substrates for phosphorylated MRS. Although the MRS SD mutant
361 showed extended affinity to a broad range of tRNAs, all tRNAs were not charged by
362 MRS under ROS stress (Netzer et al., 2009). Generally, tRNAs in charge of carrying
363 hydrophilic amino acids were preferentially used for Met-misacylation. Therefore, the
364 selection of non-cognate tRNAs for Met-misacylation and coupled Met-incorporation
365 seems to be regulated in a flexible way but within a limited range to cope with different
366 environments.

367 Our finding that cells adopt MRS-mediated mistranslation to survive under
368 ROS stress via tolerating reduced translational fidelity is unique. The sacrifice of
369 translational fidelity does not seem to cause severe side effects during the short term,
370 because cells transiently transfected with the MRS SD mutant did not show any signs of
371 apoptosis (Fig. 5B,D). Long-lasting misacylation, however, may cause adverse effects
372 on cells due to the accumulation of misfolded or inactive proteins. Consistent with this
373 expectation, stable cells expressing the MRS SD mutant showed slightly reduced
374 viability in the MTT assay (Fig. 5E). There may be a correlation between long-lasting
375 misacylation and human diseases such as cancer or degenerative diseases, and this
376 should be further studied to uncover their relationship. Nevertheless, the role of dually
377 phosphorylated MRS upon ROS stimulation is advantageous at least for a short period
378 because it can induce Met-misacylation to remove ROS and to protect protein damage
379 while maintaining cell viability.

380

381 **MATERIALS AND METHODS**

382 **Cell culture**

383 HeLa and HEK293T cells were cultured in high-glucose Dulbecco's Modified Eagle's
384 Medium (DMEM) supplemented with 10% fetal bovine serum (FBS) and 1%

385 penicillin/streptomycin at 37°C in a 5% CO₂ incubator. To establish stable HeLa cell
386 lines, cells were transfected with the pcDNA3-Myc EV, pcDNA3-Myc-MRS WT,
387 pcDNA3-Myc-MRS SA or pcDNA3-Myc-MRS SD plasmid using FuGENE HD
388 (Roche) in HeLa cells. Stable cells were selected and maintained under antibiotic
389 pressure (800 µg/ml of geneticin; Duchefa Biochemie).

390

391 **ROS induction and inhibitor treatment**

392 Cells were cultured until they reached 80% confluence. Cells were treated with 4 µM
393 sodium arsenite (Sigma) or 200 µM H₂O₂ for 4 h in DMEM with FBS (2% for short-
394 term and 5% for long-term treatment) and 1% penicillin and streptomycin. Cells were
395 pre-treated with the MAPK inhibitors SB203580 (p38 MAPK inhibitor), SP600125
396 (JNK inhibitor), and PD98059 or U0126 (ERK inhibitor) 1 h before ROS induction at a
397 concentration of 20 µM. All inhibitors were purchased from Calbiochem (Billerica). For
398 the DPI chase (Enzo), cells were pre-treated with 50 µM DPI 30 min before ROS
399 induction.

400

401 **DCFH-DA assay**

402 HEK293T cells transfected with pcDNA3-Myc EV, pcDNA3-Myc-MRS WT, pcDNA3-
403 Myc-MRS SA, or pcDNA3-Myc-MRS SD plasmids were exposed to sodium arsenite (4
404 µM) for 24 h. After treatment with 20 µM DCFH-DA (Invitrogen) (Ruiz-Ramos et al.,
405 2009) for 15 min, cells were washed twice with PBS. The DCF signals were detected
406 using a fluorescence microscope equipped with a green fluorescence filter (470 nm
407 excitation, 525 nm emission) (Nikon) to monitor intracellular ROS levels.

408

409 **Immunoblotting**

410 Cells were lysed by lysis buffer (50 mM Tris-HCl pH 7.4, 0.5% Triton X-100, 5 mM
411 EDTA, 10% glycerol and 150 mM NaCl) with phosphatase inhibitor and protease
412 inhibitor (Calbiochem) for 30 min at 4°C. After centrifugation, supernatants were
413 collected and the protein amounts were quantified by Bradford assay (BioRad). Proteins
414 extracts from the cells were separated by SDS-PAGE, transferred to PVDF membrane
415 and incubated with specific primary antibodies. Antibodies for p-Ser (Abcam), p-Thr

416 (Cell Signaling), p-Tyr (Cell Signaling), Myc (Santa Cruz), Flag (Sigma), MRS
417 (Abcam), tubulin (Sigma), DsRed (Clontech), Bax (Santa Cruz) and Bcl-2 (Santa Cruz)
418 were used in this study. Primary antibodies were used at the concentration of 0.2-0.4
419 $\mu\text{g/ml}$ (Abcam, Sigma and Santa Cruz) or with a 1:1000 dilution (Cell Signaling).

420

421 **Immunoprecipitation**

422 Protein extracts were incubated with primary antibody (2 μg) for 4 h at 4°C with
423 agitation, and then incubated further for 4 h at 4°C with protein A agarose (Invitrogen).
424 Beads were washed three times with cold lysis buffer and supernatants were removed.
425 Samples were dissolved in the SDS sample buffer and separated by SDS-PAGE.

426

427 **2D-PAGE**

428 Protein extracts from HeLa cells were incubated with alkaline phosphatase (Roche) for
429 2 h. Each 500 μg protein extract was rehydrated in resolubilization buffer (7 M urea, 2
430 M thiourea, 2% ASB-14, 0.5% Triton X-100, 1% (vol/vol) ampholyte, 1% (vol/vol)
431 tributylphosphine and 0.1% bromophenol blue). Samples were loaded onto the
432 immobilized pH gradient (IPG) strip gels (linear pH gradient 4-7, 7cm, Bio-Rad) and
433 subjected to isoelectric focusing (Bio-Rad).

434

435 ***In vitro* kinase assay and filter binding assay**

436 GST-fusion MRS proteins were purified from *Escherichia coli* Rossetta 2. Proteins were
437 induced by 0.5 mM isopropyl- β -D-thiogalactopyranoside (IPTG) and cultured at 18°C
438 for overnight. Harvested cells were lysed by sonication, and lysates were incubated with
439 glutathione Sepharose 4B (GE Healthcare) in the lysis buffer (PBS containing 0.5%
440 Triton X-100 and protease inhibitor) at 4°C for 6 h. Before the kinase reaction, the GST-
441 fusion MRS proteins were pre-incubated with 500 μM ATP for 10 min at room
442 temperature and the kinase reactions were performed at 30°C for 30 min by adding
443 ERK (Cell science), [γ - ^{32}P]ATP (IZOTOP, SBP301-1000 μCi), and kinase buffer (100
444 mM Tris-HCl pH 7.4, 75 mM MgCl_2 , 5 mM EGTA, 1 mM DTT, phosphatase inhibitor
445 and protease inhibitor). Reactions were stopped by adding the SDS sample buffer and
446 the samples were separated by SDS-PAGE gel and detected by autoradiography.

447 For the peptide kinase assay (Kwon et al., 2011), GFP-ERK expressed in
448 HEK293T cells with or without U0126 pre-treatment was immunoprecipitated with
449 anti-GFP antibody. N-terminal biotinylated peptides were chemically synthesized (GL
450 Biochem). Each peptide [3 mM MRS Ser209 (QKQPFQPSPAEGR), MRS S209A
451 (QKQPQAPAEGR), MRS Ser825 (GGQAKTSPKPA), MRS S825A
452 (GGQAKTAPKPA), positive control (APRTPGGRR), and negative control
453 (APRAPGGRR)] was reacted with the GFP-ERK at 30°C for 30 min. Soup from each
454 sample was filtered through a streptavidin-coated matrix biotin-capture membrane
455 (Promega) using a 96-well Minifold filtration apparatus. The membrane was washed
456 according to the previous report (Schaefer and Guimond, 1998) and exposed for
457 autoradiography.

458

459 **CD Spectrum analysis**

460 MBP-MRS WT and MBP-MRS SA and SD mutants were purified and eluted with a
461 buffer containing 50 mM maltose at 4°C for 24 h and then dialyzed with 10 mM
462 potassium phosphate buffer (pH 7.4). The CD spectrum was measured using a Jasco J-
463 815 CD spectrometer at 25°C and 70°C in the far-UV range from 190 to 250 nm.
464 Samples were loaded into a 1mm path-length absorption micro cell. The results are
465 shown as an average of three repeated scans after subtraction of buffer background.

466

467 **Aminoacylation assay**

468 His-tagged MRS (WT, SA and SD) expressed in *E. coli* RIL was purified using
469 ProBond Resin (Invitrogen) and washed with lysis buffer (pH7.8, 20 mM KH₂PO₄, 500
470 mM NaCl, 10% glycerol and 2 mM 2-mercaptoethanol) changing the buffer pH from
471 7.8, to 6 to 5.2, and back to 6, with 24 mM imidazole at the final step. His-MRS was
472 eluted in the presence of 300 mM imidazole (pH 6.0) and dialyzed with PBS containing
473 20% glycerol. tRNA^{Met}(CAU), tRNA^I^{Met}(CAU), tRNA^{Lys}(CUU), tRNA^{Ala}(AGC),
474 tRNA^{Gly}(GCC), tRNA^{His}(GUG) and tRNA^{Leu}(CAG) were synthesized via *in vitro*
475 transcription. MRS aminoacylation activity was performed at 37°C in reaction buffer
476 (30 mM HEPES, pH 7.4, 100 mM potassium acetate, 10 mM magnesium acetate, 4 mM
477 ATP, 20 μM Met, 500 μg/mL each tRNA, 400 nM purified MRS and 25 μCi [³⁵S]Met
478 (IZOTOP, 1000 Ci/mmol). For kinetics analysis, each tRNA (tRNA^{Met}, tRNA^I^{Met} and

479 tRNA^{Lys}) was used at the concentration from 0.5 μ M to 80 μ M. Aminoacylation
480 reaction samples were spotted on 3 MM filter paper pre-wetted with 5% trichloroacetic
481 acid (TCA) containing 1 mM Met. Washing three times with 5% TCA and dried,
482 radioactivity was detected by liquid scintillation counter (Wallac 1409).

483

484 **EMSA**

485 tRNA^{eMet}(CAU), tRNA^{Lys}(CUU), tRNA^{Ala}(AGC), tRNA^{Gly}(GCC), tRNA^{His}(GUG) and
486 tRNA^{Leu}(CAG) were synthesized via *in vitro* transcription with [α -³²P] UTP (IZOTOP,
487 3000 Ci/mmol). Purified His-tagged MRS proteins (WT and SD; 0, 1, 2 and 2 μ M) were
488 mixed with each tRNA probe in the binding buffer (20 mM Tris-HCl pH 7.4, 75 mM
489 KCl, 10 mM MgCl₂, and 5% glycerol) and incubated at 30°C for 30 min. Samples were
490 mixed with same volume of sample buffer and separated by 6.5% non-denaturing
491 polyacrylamide gel. Radioactivity was detected by autoradiography.

492

493 **Mass spectrometry analysis**

494 GST-fusion MRS domains (MD1 and MD3) were incubated with ERK and ATP, and
495 were subjected to SDS-PAGE. MRS bands were cut from the SDS-PAGE gel and in gel-
496 digested with trypsin (Promega). tryptic digests of MRS are subsequently separated by
497 online reversed-phase chromatography for each run using a Thermo Scientific Eazynano
498 LC II autosampler with a reversed-phase peptide trap EASY-Column (100 μ m inner
499 diameter, 2 cm length) and a reversed-phase analytical EASY-Column (75 μ m inner
500 diameter, 10 cm length, 3 μ m particle size, both Thermo Scientific), and electrospray
501 ionization was subsequently performed using a 30 μ m (i.d.) nano-bore stainless steel
502 online emitter (Thermo Scientific) and a voltage set at 2.6 V, at a flow rate of 300 nl/min.
503 The chromatography system was coupled on-line with an LTQ VelosOrbitrap mass
504 spectrometer equipped with an ETD source. To improve peptide fragmentation of
505 phosphopeptides, we applied a data dependent neutral loss MS3 ETD mode or a data
506 dependent decision tree (DDDT) to select for collision induced dissociation (CID) or
507 electron transfer dissociation (ETD) fragmentation depending from the charge states,
508 respectively. Protein identification was accomplished utilizing the Proteome Discoverer
509 v1.3 database search engine (Thermo scientific) and searches were performed against
510 IPI.human.v3.2 FASTA database or human MRS FASTA database. A fragment mass

511 tolerance of 1.2 Da, peptide mass tolerance of 15 ppm, and maximum missed cleavage
512 of 2 was set. Result filters was performed with peptide rank (Maximum rank: 1),
513 peptides number per protein (Minimal number of peptides: 2, Count only rank 1
514 peptides: True, Count peptide only in top scored proteins: True) and Charge State versus
515 Score (Score to which the filter is applied: Sequest Node (XCorr), Minimal Score for
516 charge state = +1: 1.7, + 2: 2.5, +3: 3.2, > +4: 3.5). The Carbamidomethylation
517 (+57.021 Da) of cystein (C) is set as a Static Modification, and the following variable
518 modification were allowed: GlyGly / +114.043 Da (K), Acetyl / +42.011 Da (K),
519 HexNAc / +203.079 Da (N, S, T), Phospho / +79.966 Da (S, T, Y), Oxidation / +15.995
520 Da (M), deamidated / +0.984 Da (N, Q). Each processed data was subsequently
521 transformed to .sf file with Scaffold 3 program and finally all MRS PTMs identified
522 from control or stimulated sample, respectively were scored and compared with
523 Scaffold PTM software.

524 For Met-misincorporation data analysis, protein identification was
525 accomplished utilizing the Proteome Discoverer v1.3 database search engine (Thermo
526 scientific) and searches were performed against Flag-VN-AIMP3 FASTA database. The
527 carbamidomethylation (+57.021 Da) of cystein (C) or deamidated (+0.984 Da) of
528 asparagine or glutamine (N, Q) is set as a static modification or as a variable
529 modification, respectively. To identify the exchange of specific amino acid to Met, the
530 following variable modification was additionally allowed; K→M/ +2.946 Da (K),
531 D→M / +16.014 Da (D), V→M / +31.972 Da (V), G→M / +74.019 Da (G), H→M /
532 -6.018 Da (H), L→M / +17.956 Da (L), A→M / +60.003 Da (A) and Oxidation /
533 +15.995 Da (M). Finally all Flag-VN-AIMP3 PTMs identified from both conditions
534 were manually inspected.

535

536 **Met-misincorporation detection by radioisotope**

537 HEK293T cells were transfected with pBiFC-VN173-AIMP3 and pcDNA3-Myc EV or
538 pcDNA3-Myc-MRS (WT, SA or SD) plasmids using Fugene HD transfection reagent
539 (Roche). After 24 h, the cells were treated with 50 μ M ALLN in DMEM methionine
540 free media (Invitrogen) for 30 min. To confirm the effect of ERK on MRS-mediated
541 mismethionylation, ERK inhibitor was co-treated with ALLN. Then 1 mCi [³⁵S]Met
542 was added to the cells and incubated for 2 h. Cells were further incubated with 4 μ M

543 sodium arsenite for 4 h, washed twice with PBS and then subjected to
544 immunoprecipitation. After SDS PAGE, the [³⁵S]Met incorporation into the Flag-
545 AIMP3 protein was detected by autoradiography.

546

547 **TagRFP mutant generation and Met-misincorporation detection by fluorescence**

548 PCR-based site-directed mutagenesis was performed to change Met67 in TagRFP
549 (GenBank: BAI43881.1) to Lys (M67K), His (M67H) and Gly (M67G). Briefly, Hind
550 III fragment in pHAG016 in which TagRFP was cloned after SR α promoter was
551 swapped with Hind III digests of PCR fragments containing mutations in the 3' PCR
552 primer region.

553 Each TagRFP plasmid was co-transfected with pcDNA3-Myc EV or pcDNA3-Myc-
554 MRS (WT, SA and SD) into the HEK293 cells. After 24 h, the cells were treated with
555 4 μ M arsenite-treated and incubated for 4 h. Images were analyzed for snap pictures
556 using MetaMorph software. The red fluorescent cells were counted using 3 randomly
557 selected scopes in high-power fields (x20). Because of differences in the light
558 absorption rate, light path, and material properties of cell culturing gels, the brightness
559 is not uniform over the microscopic image. Non-uniform illumination correction is
560 required as pre-processing before image analysis.

561 To analysis cell images based on fluorescence intensity, image contrast was
562 adjusted using a localized version of the modification framework histogram smoothing
563 (MF-HS) algorithm (Arici et al., 2009) to enhance the low-dynamic input image without
564 producing over-enhancing artifacts in the resulting image. Then, the advanced simple
565 linear iterative clustering (SLIC) superpixels method as used for cell segmentation. To
566 identify the approximate boundary of cell, the degree of initial size and compactness
567 parameters were used. Interested cell region was manually selected after SLIC
568 superpixel method. The feature vectors were extracted from the selected cell object and
569 used to analyze the differences in cell size and intensity.

570

571 **Cell growth and viability assay**

572 Stable HeLa cells expressing pcDNA3-Myc EV or pcDNA-Myc-MRS (WT, SA and
573 SD) were treated with 4 μ M sodium arsenite and the cell growth curve was monitored at
574 37°C for 48 h using IncuCyte Kinetic Live Cell Imaging System (Essen BioScience).

575 To assess the cell viability, MTT (USB) stock solution (5 mg/ml) was added to a final
576 concentration of 0.5 mg/ml in each well containing 200 μ l medium and incubated for 30
577 min. The precipitated crystal was dissolved in 100 μ l of DMSO (Sigma). Absorbance
578 was measured at 450 nm using microplate reader (Sunrise, TECAN).

579

580 **TUNEL assay**

581 Stable HeLa cells expressing pcDNA3-Myc EV or pcDNA-Myc-MRS (WT, SA and
582 SD) were treated with 4 μ M sodium arsenite for 72 h and apoptosis was measured using
583 Dead End Fluorometric TUNEL assay system (Promega) according to the
584 manufacturer's manual. ERK inhibitor was pre-treated 1 h before arsenite treatment
585 when required.

586

587 **Statistical analysis**

588 Statistical significance of data was determined by applying Student's *t* test or analysis.
589 Significance of analysis of variance is indicated in the figures as *, $P < 0.05$; **, $P < 0.01$;
590 and ***, $P < 0.001$. Statistics were calculated with the Prism 5 software (GraphPad
591 Software).

592

593 **Acknowledgments**

594 We thank to Dr. T. Pan and Dr. T. Jones (University of Chicago) for the discussion.

595

596 **Competing interests**

597 The authors declare that they have no competing interests.

598

599 **Author contributions**

600 N.H.K. and S.K. conceived the project, and designed the experiments. J.Y.L., N.H.K.
601 and S.K. drafted the manuscript. J.Y.L., D.G.K., B.G.K., W.S.Y., J.H., T.K., Y.S.O.,
602 K.R.K., B.W.H., B.J.H., M.S.K., M.H.K. and N.H.K. performed the experiments and
603 analyzed and interpreted the data. All authors contributed to discussion.

604

605 **Funding**

606 This work was supported by the Global Frontier Project grants (NRF-M3A6A4-2010-

607 0029785 [S.K.], NRF-2013M3A6A4045452 [B.J.H.], NRF-2013-045813 [B.S.K]) of
608 National Research Foundation funded by the Ministry of Science, ICT & Future
609 Planning (MSIP) of Korea, and by the Korea Science & Engineering Foundation
610 through the Acceleration Research Program (NRF-2008-0060617 [M.H.K]). This study
611 was also funded by a grant from Gyeonggi Research Development Program [S.K.].
612 MRS purification was supported by the National R&D Program for Cancer Control
613 (Grant number 1120170) from National Cancer Center of Korea.

614

615 **Supplementary material**

616 Supplementary material is available online.

617

618 **References**

- 619 **Arci, T., Dikbas, S. and Altunbasak, Y.** (2009) A histogram modification framework and its
620 application for image contrast enhancement. *IEEE Trans. Image Process* **18**, 1921-1935.
- 621 **Birben, E., Sahiner, U. M., Sackesen, C., Erzurum, S. and Kalayci, O.** (2012) Oxidative stress
622 and antioxidant defense. *World Allergy Organ. J.* **5**, 9-19.
- 623 **Chen, Y. C., Lin-Shiau, S. Y. and Lin, J. K.** (1998) Involvement of reactive oxygen species and
624 caspase 3 activation in arsenite-induced apoptosis. *J. Cell. Physiol.* **177**, 324-333.
- 625 **Englich, S., Englich, U., von der Haar, F. and Cramer, F.** (1986) The proofreading of hydroxy
626 analogues of leucine and isoleucine by leucyl-tRNA synthetases from *E. coli* and yeast.
627 *Nucleic Acids Res.* **14**, 7529-7539.
- 628 **Fersht, A. R. and Dingwall, C.** (1979) An editing mechanism for the methionyl-tRNA synthetase
629 in the selection of amino acids in protein synthesis. *Biochemistry* **18**, 1250-1256.
- 630 **Fleury, C., Mignotte, B. and Vayssiere, J. L.** (2002) Mitochondrial reactive oxygen species in cell
631 death signaling. *Biochimie* **84**, 131-141.
- 632 **He, R., Zu, L. D., Yao, P., Chen, X. and Wang, E. D.** (2009) Two non-redundant fragments in
633 the N-terminal peptide of human cytosolic methionyl-tRNA synthetase were indispensable for
634 the multi-synthetase complex incorporation and enzyme activity. *Biochim. Biophys. Acta* **1794**,
635 347-354.
- 636 **Hossain, K., Akhand, A. A., Kato, M., Du, J., Takeda, K., Wu, J., Takeuchi, K., Liu, W., Suzuki,
637 H. and Nakashima, I.** (2000) Arsenite induces apoptosis of murine T lymphocytes through
638 membrane raft-linked signaling for activation of c-Jun amino-terminal kinase. *J. Immunol.* **165**,
639 4290-4297.
- 640 **Jakubowski, H.** (1991) Proofreading in vivo: editing of homocysteine by methionyl-tRNA
641 synthetase in the yeast *Saccharomyces cerevisiae*. *The EMBO journal* **10**, 593-598.

- 642 **Jones, Q. R., Warford, J., Rupasinghe, H. P. and Robertson, G. S.** (2012) Target-based
643 selection of flavonoids for neurodegenerative disorders. *Trends Pharmacol. Sci.* **33**, 602-610.
- 644 **Jones, T. E., Alexander, R. W. and Pan, T.** (2011) Misacylation of specific nonmethionyl tRNAs
645 by a bacterial methionyl-tRNA synthetase. *Proc. Natl. Acad. Sci. USA* **108**, 6933-6938.
- 646 **Kaminska, M., Shalak, V. and Mirande, M.** (2001) The appended C-domain of human
647 methionyl-tRNA synthetase has a tRNA-sequestering function. *Biochemistry* **40**, 14309-14316.
- 648 **Kwon, N. H., Kang, T., Lee, J. Y., Kim, H. H., Kim, H. R., Hong, J., Oh, Y. S., Han, J. M., Ku, M.**
649 **J., Lee, S. Y. et al.** (2011) Dual role of methionyl-tRNA synthetase in the regulation of
650 translation and tumor suppressor activity of aminoacyl-tRNA synthetase-interacting
651 multifunctional protein-3. *Proc. Natl. Acad. Sci. USA* **108**, 19635-19640.
- 652 **Lau, A. T., Li, M., Xie, R., He, Q. Y. and Chiu, J. F.** (2004) Opposed arsenite-induced signaling
653 pathways promote cell proliferation or apoptosis in cultured lung cells. *Carcinogenesis* **25**, 21-
654 28.
- 655 **Levine, R. L., Mosoni, L., Berlett, B. S. and Stadtman, E. R.** (1996) Methionine residues as
656 endogenous antioxidants in proteins. *Proc. Natl. Acad. Sci. USA* **93**, 15036-15040.
- 657 **Levine, R. L., Moskovitz, J. and Stadtman, E. R.** (2000) Oxidation of methionine in proteins:
658 roles in antioxidant defense and cellular regulation. *IUBMB life* **50**, 301-307.
- 659 **Luo, S. and Levine, R. L.** (2009) Methionine in proteins defends against oxidative stress.
660 *FASEB journal : official publication of the Federation of American Societies for Experimental*
661 *Biology* **23**, 464-472.
- 662 **Netzer, N., Goodenbour, J. M., David, A., Dittmar, K. A., Jones, R. B., Schneider, J. R., Boone,**
663 **D., Eves, E. M., Rosner, M. R., Gibbs, J. S. et al.** (2009) Innate immune and chemically
664 triggered oxidative stress modifies translational fidelity. *Nature* **462**, 522-526.
- 665 **Pan, J. S., Hong, M. Z. and Ren, J. L.** (2009) Reactive oxygen species: a double-edged sword
666 in oncogenesis. *World J. Gastroenterol.* **15**, 1702-1707.
- 667 **Park, S. G., Ewalt, K. L. and Kim, S.** (2005) Functional expansion of aminoacyl-tRNA
668 synthetases and their interacting factors: new perspectives on housekeepers. *Trends*
669 *Biochem. Sci.* **30**, 569-574.
- 670 **Pendergast, A. M. and Traugh, J. A.** (1985) Alteration of aminoacyl-tRNA synthetase activities
671 by phosphorylation with casein kinase I. *J. Biol. Chem.* **260**, 11769-11774.
- 672 **Ruiz-Ramos, R., Lopez-Carrillo, L., Rios-Perez, A. D., De Vizcaya-Ruiz, A. and Cebrian, M. E.**
673 (2009) Sodium arsenite induces ROS generation, DNA oxidative damage, HO-1 and c-Myc
674 proteins, NF-kappaB activation and cell proliferation in human breast cancer MCF-7 cells.
675 *Mutat. Res.* **674**, 109-115.
- 676 **Schaefer, E. M. and Guimond, S.** (1998) Detection of protein tyrosine kinase activity using a
677 high-capacity streptavidin-coated membrane and optimized biotinylated peptide substrates.
678 *Anal. Biochem.* **261**, 100-112.

- 679 **Senger, B., Despons, L., Walter, P. and Fasiolo, F.** (1992) The anticodon triplet is not sufficient
680 to confer methionine acceptance to a transfer RNA. *Proc. Natl. Acad. Sci. USA* **89**, 10768-
681 10771.
- 682 **Son, Y., Cheong, Y. K., Kim, N. H., Chung, H. T., Kang, D. G. and Pae, H. O.** (2011) Mitogen-
683 Activated Protein Kinases and Reactive Oxygen Species: How Can ROS Activate MAPK
684 Pathways? *J. Signal Transduct.* **2011**, 792639.
- 685 **Stadtman, E. R., Moskovitz, J., Berlett, B. S. and Levine, R. L.** (2002) Cyclic oxidation and
686 reduction of protein methionine residues is an important antioxidant mechanism. *Molecular*
687 *and cellular biochemistry* **234-235**, 3-9.
- 688 **Stadtman, E. R., Moskovitz, J. and Levine, R. L.** (2003) Oxidation of methionine residues of
689 proteins: biological consequences. *Antioxidants & redox signaling* **5**, 577-582.
- 690 **Trachootham, D., Alexandre, J. and Huang, P.** (2009) Targeting cancer cells by ROS-mediated
691 mechanisms: a radical therapeutic approach? *Nat. Rev. Drug Discov.* **8**, 579-591.
- 692 **Waris, G. and Ahsan, H.** (2006) Reactive oxygen species: role in the development of cancer
693 and various chronic conditions. *J. Carcinog.* **5**, 14.
- 694 **Wiltrout, E., Goodenbour, J. M., Frechin, M. and Pan, T.** (2012) Misacylation of tRNA with
695 methionine in *Saccharomyces cerevisiae*. *Nucleic Acids Res.* **40**, 10494-10506.
- 696 **Yadavalli, S. S. and Ibba, M.** (2012) Quality control in aminoacyl-tRNA synthesis its role in
697 translational fidelity. *Adv. Protein Chem. Struct. Biol.* **86**, 1-43.
- 698
- 699
- 700
- 701
- 702
- 703
- 704
- 705
- 706
- 707
- 708
- 709
- 710
- 711
- 712
- 713

714 **Table 1. Comparison of catalytic activities between MRS WT, SA and SD.**

Enzyme	Constants	Met-tRNA ^e _{Met}	Met-tRNA ⁱ _{Met}	Met-tRNA ^{Lys}
WT	K _M (μM)	3.03 ± 0.063	5.515 ± 0.0768	N.D
	k _{cat} (s ⁻¹)	0.157 ± 0.002	0.0176 ± 0.00009	N.D
	k _{cat} /K _M (μM ⁻¹ s ⁻¹)	0.051 ± 0.042	0.00319 ± 0.00004	N.D
SD	K _M (μM)	41.83 ± 14.19	7.616 ± 0.195	25.56 ± 4.94
	k _{cat} (s ⁻¹)	0.127 ± 0.052	0.0155 ± 0.000111	0.089 ± 0.0045
	k _{cat} /K _M (μM ⁻¹ s ⁻¹)	0.0031 ± 0.0002	0.002 ± 0.00003	0.0035 ± 0.0004
SA	K _M (μM)	7.96 ± 2.84	8.3003 ± 0.4264	N.D
	k _{cat} (s ⁻¹)	0.011 ± 0.0005	0.0143 ± 0.0002	N.D
	k _{cat} /K _M (μM ⁻¹ s ⁻¹)	0.0015 ± 0.0005	0.00172 ± 0.00006	N.D

715

716 Catalytic activities of WT MRS and the SD and SA mutants were measured using
 717 tRNA^e_{Met}(CAU), tRNAⁱ_{Met}(CAU) and tRNA^{Lys}(CUU) to obtain kinetic parameters (K_M,
 718 k_{cat} and k_{cat}/K_M values). tRNAs were used in the concentration range of 0.5–80 μM.
 719 Data are represented as mean ± s.d. (*n* = 3). N.D., not detected.

720

721

722

723

724

725

726

727

728

729

730

731

732

733

734

735 **Table 2. Met-misincorporated residues in Flag-VN-AIMP3.**

Target	Sequence	Site
FLAG-Venus N-term	GEELFTGVVPILVELDGDVNGHK	D20, D22
	GEELFTGVVPILVELDGDVNGHK	V23
	FSVSGEGEGDATYGK	D37
	LPVPWPTLVTTLG YGLQCFAR	V56
	FEGDTLVNRIELK	G117
	LEYNYNSHNVYITADKQK	V151
	EDGNILGHKLEYNYNSHNVYITADKQK	K157
AIMP3	ANFKIRHNIEMAAAELSLEK	A2, A4, A5
	HNIEMAAAELSLLEKSLGLSK	L7, L9
	SLGLSKGNKYSAQGER	K21
	QANKEYLLGSTAEEKAIVQQWLEYR	K57

736

737 Peptide sequences detected by mass spectrometry analysis. Red color indicates the
 738 residues identified only from the HEK293T cells expressing the MRS SD mutant.
 739 Orange color indicates the residues detected from HEK293T cells expressing WT MRS
 740 under normal condition as well as cells expressing the MRS SD mutant.

741

742

743

744

745

746

747

748

749

750

751

752

753

754 **FIGURE LEGENDS**

755 **Fig. 1. Determination of ERK-mediated phosphorylation sites in MRS under ROS**

756 **stress.** (A) Lysates from untreated and sodium arsenite-treated HeLa cells were
757 subjected to 2D-PAGE. The gel was immunoblotted with anti-MRS antibody. To check
758 ROS-dependent phosphorylation of MRS, lysates from sodium arsenite-treated cells
759 were incubated with alkaline phosphatase (AP). (B) Lysates prepared as above were
760 immunoprecipitated with anti-MRS antibody and immunoblotted with phosphoserine
761 (p-Ser), phosphothreonine (p-Thr), and phosphotyrosine (p-Tyr) specific antibodies. (C)
762 Lysates from HeLa cells treated with sodium arsenite with or without DPI (ROS
763 inhibitor) were immunoprecipitated using anti-MRS antibody. The gel was
764 immunoblotted with p-Ser antibody. (D) HeLa cells pre-treated with each MAPK
765 inhibitor, SB203580 (p38 MAPK), SP600125 (JNK) and PD98059 (ERK), were
766 incubated in sodium arsenite-containing media. The lysates were immunoprecipitated
767 with anti-MRS antibody and immunoblotted with p-Ser antibody. (E) Purified GST (EV,
768 empty vector) and GST-MRS was subjected to an *in vitro* kinase reaction by incubating
769 with ERK and [γ -³²P]ATP. After staining with coomassie brilliant blue, radioactivity
770 was detected by autoradiography. (F) Schematic representation of functional domains in
771 human MRS. The domains of MRS can be divided into MD1 (GST-like, residues 1–
772 266), MD2 (Catalytic, residues 267–597) and MD3 (tRNA-binding, residues 598–900)
773 fragments. (G) Individual GST-fused domains of MRS were subjected to *in vitro* kinase
774 assay with ERK in the presence of [γ -³²P]ATP. Phosphorylation signal was detected by
775 autoradiography. (H) HEK293T cells transfected with GFP-ERK were
776 immunoprecipitated with anti-GFP antibody. The immunoprecipitated GFP-ERK was
777 mixed with each biotinylated synthetic peptide (WT, wild type; SA, phosphorylation-
778 inactive form) and [γ -³²P]ATP. A consensus sequence phosphorylated by ERK was used
779 as a control (P, positive control; N, phosphorylation-inactive form of positive control)
780 (left). Positive control peptide and peptides containing each S209 and S825 were
781 incubated with [γ -³²P]ATP and immunoprecipitated ERK from U0126 pre-treated cells.
782 Autoradioactivity from the peptides was detected after dot blotting (right). (I) To
783 confirm the ERK-dependent phosphorylation sites in MRS, *in vitro* kinase assay was
784 performed with WT GST-MRS and the GST-MRS S209A/S825A (SA) mutant as
785 described above. The phosphorylation signal was detected by autoradiography. The

786 relative quantification obtained by densitometer analysis for the phosphorylation signal
787 of WT MRS and SA mutant was 1 and 0.11, respectively. (J) HEK293T cells transfected
788 with Myc-MRS WT or Myc-MRS SA mutant were treated with sodium arsenite and
789 immunoprecipitated using anti-Myc antibody. Arsenite-dependent phosphorylation of
790 MRS was detected using the p-Ser antibody.

791

792 **Fig. 2. Dually phosphorylated MRS undergoes a conformational change and binds**
793 **to tRNA^{Lys}(CUU).** (A) Maltose-binding protein (MBP) tagged WT MRS and the MBP-
794 MRS SA and SD mutants were purified and the CD spectra of these proteins were
795 obtained in the far-UV at two different temperatures (left). The purified proteins were
796 run using SDS-PAGE and stained with coomassie brilliant blue (right). (B) Binding
797 affinities of WT MRS and the S209D/S825D (SD) mutant to tRNA^{Lys}(CUU) (top) and
798 tRNA^{Met}(CAU) (bottom) were determined by the electrophoretic mobility shift assay.
799 Each tRNA probe was incubated with WT His-MRS and His-MRS SD mutant proteins
800 and separated by non-denaturing PAGE.

801

802 **Fig. 3. Dually phosphorylated MRS induces mismethylation under ROS stress.**
803 (A) HEK293T cells were transfected with WT TagRFP or the TagRFP M67K mutant
804 and the fluorescence of each protein was compared. Insets show the same field as in
805 the phase-contrast image. Scale bar = 80 μ m (left). The expression level of WT TagRFP
806 and the TagRFP M67K mutant were determined by immunoblotting (right). (B-E) MRS-
807 dependent Met-misincorporation was monitored using the TagRFP M67K mutant whose
808 fluorescence disappeared due to the M to K substitution. HEK293T cells co-transfected
809 with Tag-RFP M67K and EV or each type of Myc-MRS (WT, SA or SD mutant) were
810 treated with sodium arsenite. Revival of fluorescence due to Met-misincorporation at
811 the M67K residue position was observed by fluorescence microscopy ($\times 200$).
812 Insets show the same field as in the phase-contrast images. Scale bar = 80 μ m (B).
813 Expression levels of total MRS, Myc-MRS (WT, SA or SD mutant) and TagRFP M67K
814 mutant were analyzed via immunoblotting (C). The relative number (D) and the relative
815 fluorescence intensity (E) of red fluorescent cells are presented as a bar graph. Data are
816 represented as mean \pm s.d. ($n = 3$). ***, $P < 0.001$; **, $P < 0.01$. a, P value indicates a
817 significant difference between the arsenite-untreated and -treated groups; b, P value

818 indicates a significant difference between arsenite-untreated EV and SD groups. (F)
819 HEK293T cells transfected with Flag-VN-AIMP3 were incubated with arsenite,
820 [³⁵S]Met and with or without ERK inhibitor, U0126. The radioactive signal from the
821 immunoprecipitated Flag-VN-AIMP3 was detected by autoradiography. (G) HEK 293T
822 cells co-transfected with Flag-VN-AIMP3 and EV or each type of Myc-MRS (WT, SA
823 or SD mutant) were incubated with [³⁵S]Met in the presence with arsenite. To see the
824 effect of ERK inhibitor, cells were pre-treated with U0126 1 h before the arsenite
825 treatment. The cell extracts were immunoprecipitated with anti-Flag antibody. [³⁵S]Met
826 signals from the Flag-VN-AIMP3 were monitored by autoradiography.

827

828 **Fig. 4. Met-misincorporated residues in Flag-VN-AIMP3 and their location in the**
829 **AIMP3 and Venus structures.** (A,B) The Met-exchanged residues identified by mass
830 spectrometry analysis were depicted in the AIMP3 (pdb2uz8) (A) and the full Venus
831 (pdb3t6h) (B) structures, respectively. Residues only identified from HEK293T cells
832 expressing WT MRS (A,B top) and MRS SD (A,B middle) are depicted in cyan and red,
833 respectively. Common residues identified from both cells are represented in orange. The
834 original Met residue in AIMP3 is depicted in green. Mismethionylated residues on
835 AIMP3 in SD-overexpressing conditions are also represented on the MRS-AIMP3
836 complex structure (pdb4bl7) (A, bottom). The GST-domain of MRS is shown in light
837 green. Each VN and VC (deleted C-terminus of Venus) in the full Venus protein
838 structure is shown in green and red, respectively, for convenience (B, bottom).

839

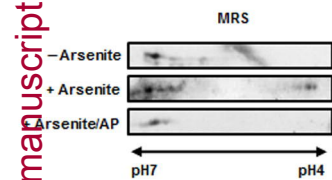
840 **Fig. 5. Dually phosphorylated MRS reduces intracellular ROS levels and promotes**
841 **cell survival under ROS stress.** (A) HEK293T cells were transfected with EV or Myc-
842 tagged WT MRS, or the SA or SD mutants, and incubated with arsenite. ROS levels
843 were detected by the DCFH-DA assay. Insets show the same field as in the phase-
844 contrast images. Scale bar = 200 μm. (B) Bax and Bcl-2 levels were detected with their
845 specific antibodies under the same conditions as shown in (A). Exogenous and
846 endogenous MRS were separated and detected using MRS antibody to show the
847 expression level. (C) MRS level in HEK293T cells was reduced by si-MRS treatment
848 for 72 h. The effect of MRS expression on cell viability under ROS stress was
849 determined by the MTT assay. (D and E) The effect of MRS proteins on cell viability

850 under ROS stress was determined by the MTT assay. MRS proteins were transiently
851 expressed in HEK293T cells (D) and stably expressed in HeLa cells (E). The values of
852 relative cell viability in (C) (D) and (E) are represented as mean \pm s.d. ($n = 3$). *,
853 $P < 0.05$; ***, $P < 0.001$. a, P value indicates a significant difference between the arsenite-
854 untreated and -treated groups; b, P value indicates a significant difference between
855 arsenite-treated si-control and si-MRS groups. (F) The growth curves of MRS-
856 expressing stable HeLa cells were monitored in the presence and absence of ROS stress.
857 The values of relative cell growth are represented as mean \pm s.d. ($n = 3$). (G) ROS-
858 dependent apoptosis was determined in MRS-expressing stable HeLa cells using the
859 TUNEL assay. Cells incubated with or without arsenite for 72 h were fixed and stained
860 with 4',6-diamidino-2-phenylindole (DAPI; blue) and fluorescein-labeled dUTP. Green
861 fluorescence indicates TUNEL-positive cells. Scale bar = 200 μm (top). The number of
862 TUNEL-positive cells was normalized to that of DAPI-positive cells, and the
863 quantitative analysis is represented as mean \pm s.d. ($n = 3$) (bottom). **, $P < 0.01$; ***,
864 $P < 0.001$. (H) HeLa cells expressing WT MRS were supposed to TUNEL assay as
865 described in (G) with or without U0126 pre-treatment, and the images (top) and the
866 quantitative analysis (bottom) for positive cells are present. *, $P < 0.05$; **, $P < 0.01$.

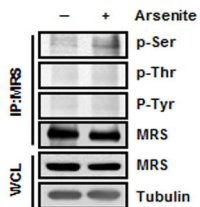
867

868 **Fig. 6. Schematic model for the protective role of MRS under ROS stress.** Upon
869 ROS stress, ERK is activated and it phosphorylates MRS at the Ser209 and Ser825
870 residues. Phosphorylated MRS enhances the mischarging of Met on non-methionyl
871 tRNAs, such as tRNA^{Lys}. Met carried by non-cognate tRNAs is incorporated into
872 growing polypeptides during translation and used as a ROS scavenger, protecting cells
873 from oxidative damage and apoptosis.

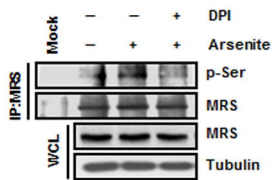
A



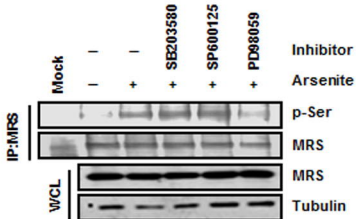
B



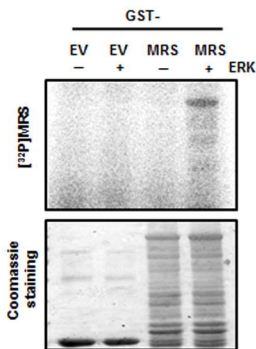
C



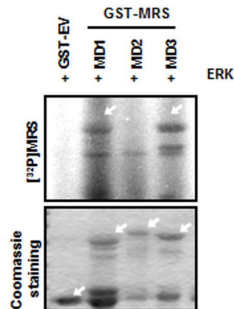
D



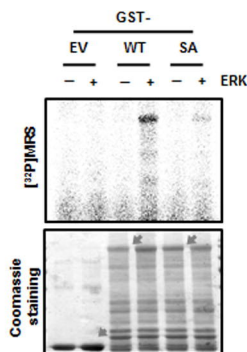
E



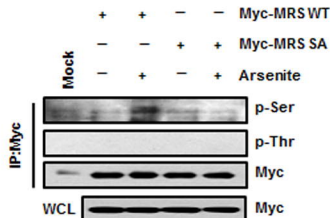
G



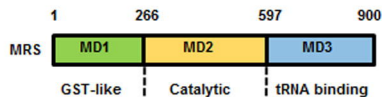
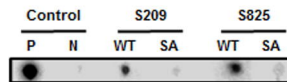
I

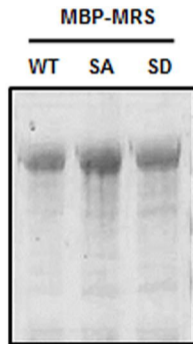
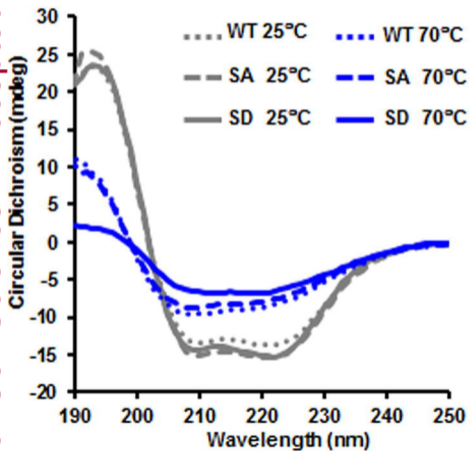
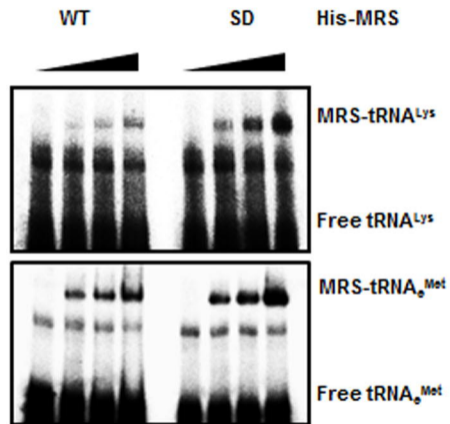


J

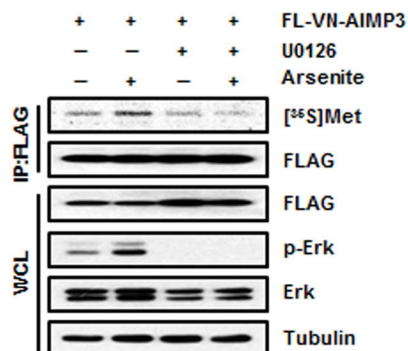
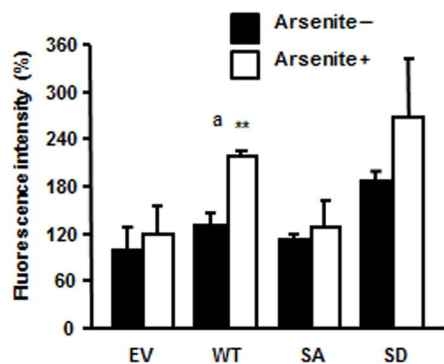
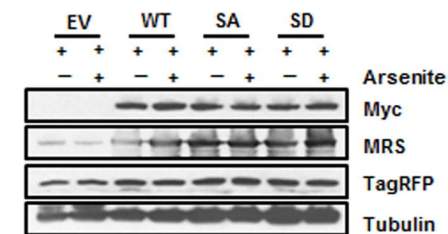
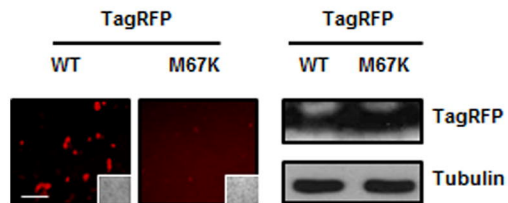


H

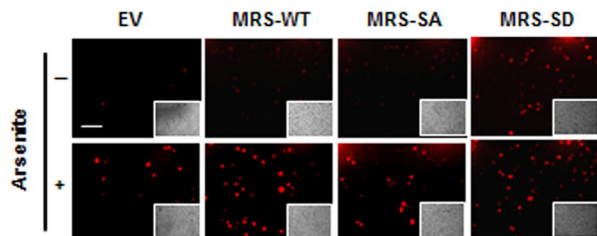


**B**

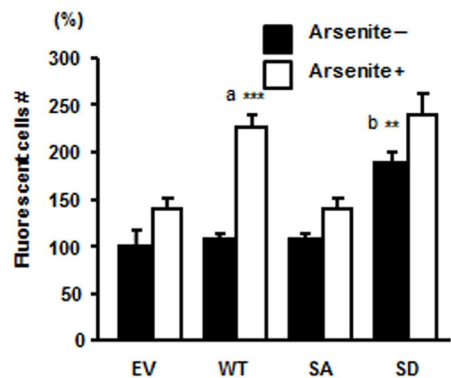
A



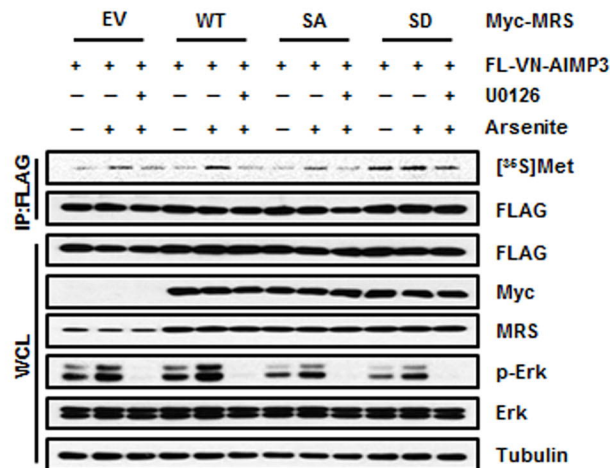
B

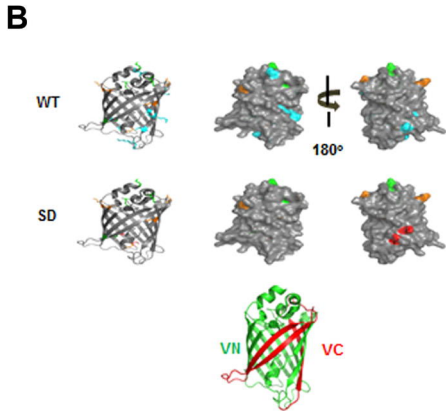
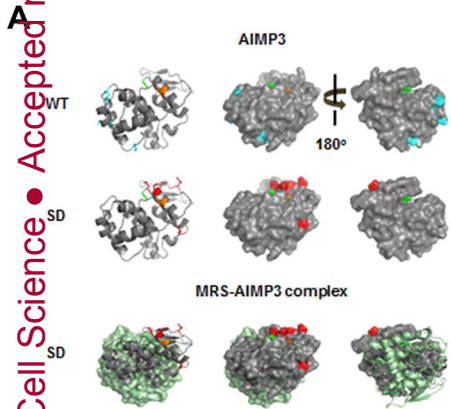


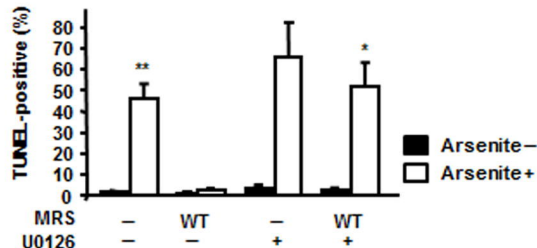
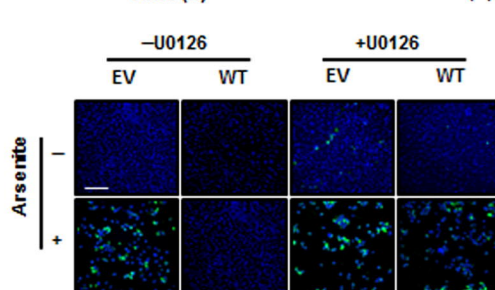
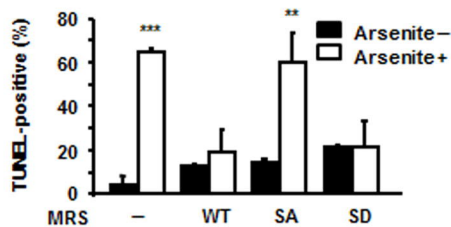
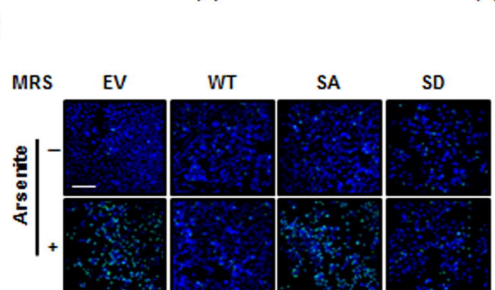
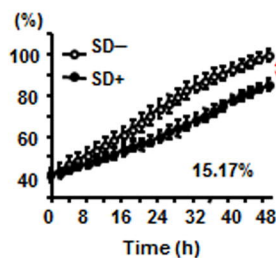
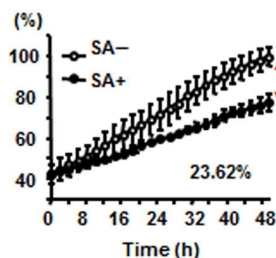
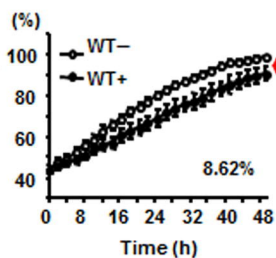
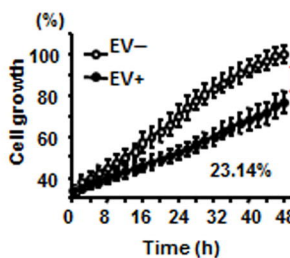
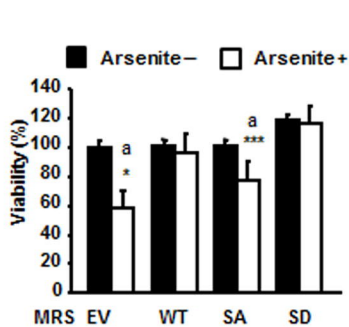
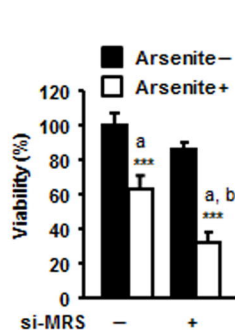
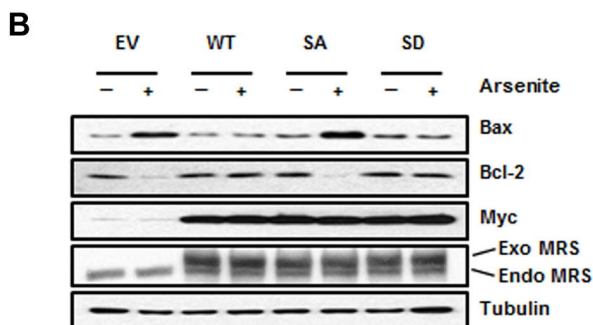
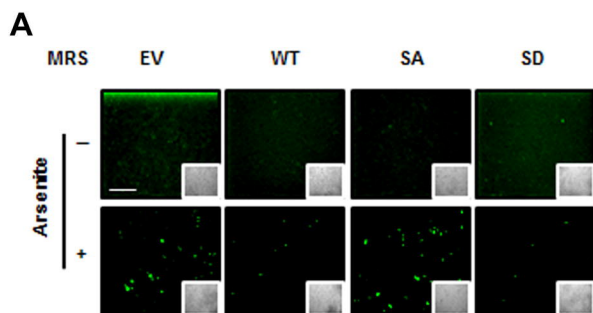
D



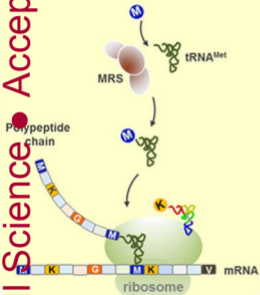
G







Methionylation Under normal condition



Adaptive mismethionylation under ROS stress

